Granular Matter manuscript No.
(will be inserted by the editor)

A.A. Peña · R. García-Rojo · H. J. Herrmann

Influence of particle shape on sheared dense granular media

Received:

Abstract We study by means of molecular dynamics simulations of periodic shear cells, the influence of particle shape on the global mechanical behavior of dense granular media. Results at macro-mechanical level show that for large shear deformation samples with elongated particles, independent of their initial orientation, reach the same stationary value for both shear force and void ratio. At the micro-mechanical level the stress, the fabric and the inertia tensors of the particles are used to study the evolution of the media. In the case of isotropic particles the direction of the principal axis of the fabric tensor is aligned with the one of the principal stress, while for elongated particles the fabric orientation is strongly dependent on the orientation of the particles. The shear band width is shown to depend on the particle shape due to the tendency of elongated particles to preferential orientations and less rotation.

Keywords Granular media · Anisotropy · Particle shape · Contact network · Shear cell

1 Introduction

Granular materials present a complex mechanical response when subjected to an external load. This global response is strongly dependent on the discrete character of the medium. The shape, angularity and size distribution of the grains, the evolution of the granular skeleton (spatial arrangement of particles, void ratio, fabric, force chains), and some phenomena occurring at the grain scale (like rolling or sliding) are determinant factors for the overall macroscopic response.

A.A. Peña · R. García-Rojo · H. J. Herrmann
Institute for Computer Applications 1,
Pfaffenwaldring 27,
70569 Stuttgart, GERMANY
E-mail: andres@ica1.uni-stuttgart.de

H. J. Herrmann
Departamento de Fisica, Universidade Federal do Ceará,
Campus do Pici, 60451-970 Fortaleza CE, Brazil

The study of anisotropy is of fundamental importance in order to understand the properties of granular materials. In soil mechanics, Casagrande and Carrillo [1] distinguished between inherent and induced anisotropy, the first as a result of the sedimentation of particles and the second as a product of inelastic deformation. Oda [2] studied by means of optical microscopic photographs of thin sections of sand, the preferred orientations and spatial relation of the constituting grains, and found that independent of their shape particles tend to rest in a stable configuration relative to the forces acting on them. Furthermore, he also found that the initial fabric is not only determined by the shape of the particles but also by the deposition or compaction method.

In relation to inherent anisotropy Oda et al. [3] and Oda and Nakayama [4] have listed three sources in such materials:

1. Anisotropic distribution of contacts (called structural anisotropy).
2. Shape and preferred orientation of void spaces.
3. Shape of the particles and preferred orientation of non-spherical ones.

The complete alteration of inherent anisotropy due to types 1 and 2 during early stages of inelastic deformation in biaxial compression tests, on two-dimensional assemblies of rods, was observed by Oda et al. [3]. They found, however, that the one due to type 3 was still present at large deformations. It would be therefore expected that in the so-called critical state of soil mechanics, which is associated with large shear deformation, the persistence of inherent anisotropy is mainly due to particle orientation [5].

The role of anisotropy in granular materials has been widely investigated both experimentally and with numerical simulations. In relation to particle shape, a big effort has been recently done to properly characterize particle geometry and to study its effect on the mechanical response of granular media. Concerning particle shape characterization Bowman et al. [6] proposed a experimental technique using fourier descriptors and image

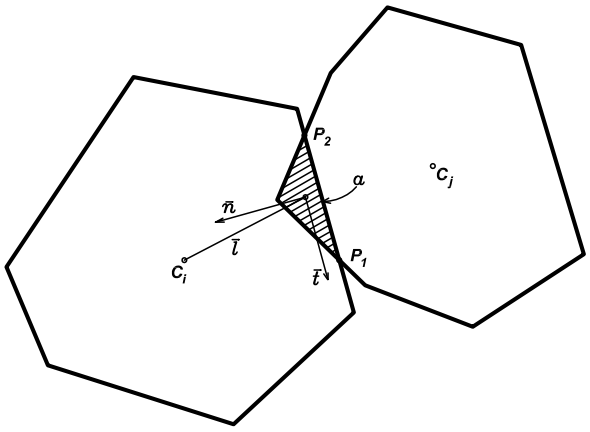

Fig. 1 Schematic representation of a particle contact, the overlapping area a is indicated by the shaded zone.

analysis to assess particle morphology and texture, and in discrete element simulations (DEM) Matsushima and Saomoto [7] presented a method to construct irregularly-shaped grains from shape data of real granular material. Regarding the influence of particle shape on the mechanical behavior of the granular media, Bowman and Soga [8] found that the stress-strain and creep response of fine silica sand is influenced by particle elongation or aspect ratio. Using two dimensional DEM simulations Shodja and Nezami [9] and Nouguier-Lehon and Frossard [10] studied the effect of particle elongation on the rolling and sliding mechanisms in granular media. Nouguier-Lehon et al. [11] studied in biaxial test simulations the influence of particle shape on the so-called critical state, and Peña et al. [12] the effect on the asymptotical states of granular media. Three dimensional studies using ellipsoidal convex-shaped particles have also been performed highlighting the role of particle shape [13; 14].

The temporal and spatial evolution of anisotropic granular materials during compaction has also been investigated. Villarruel et al. [15] found experimentally clear evidence that particle anisotropy can drive ordering (configuration of particles evolves to a nematic state). Lumay and Vandewalle [16] in experiments and simulations observed large variations of the asymptotic packing volume fraction as a function of the aspect ratio of the particles. Ribière [17] using rice of different shapes found that grain anisotropy slows down the packing fraction evolution, and that the convection in the granular media and therefore the compaction mechanism depend also on it.

The anisotropic network of contact forces in a granular packing subjected to shear conditions has been recently investigated by Majmudar and Behringer [18] in a two dimensional system of photoelastic discs and by Lätzel et al. [19] in discrete element simulations.

Up to now, however, there is no clear information at the micro-mechanical level about the influence of particle shape and the orientation of non-spherical particles on the evolution of granular materials and the corresponding anisotropic network of contacts towards the stationary state reached at the global level under shear conditions. These subjects are very important in geotechnical engineering and physics in order to get a better understanding of the mechanical response of granular materials. In this work, we use the molecular dynamics technique to simulate the mechanical behavior of two-dimensional particle assemblies contained in a periodic shear cell. The grains are represented by randomly generated convex polygons. We focus on the influence of particle shape on the overall plastic response. The dependency of the mechanical behavior on the evolution of inherent anisotropy (specially contact and non-spherical particle orientations) is studied. Results are analyzed from the macro and micro-mechanical point of view.

2 Model, sample construction and numerical experiment

2.1 Molecular dynamics simulations

We study dense polygonal packings, in which particles interact through visco-elastic contacts. The polygons can neither break nor deform, but they can overlap when they are pressed against each other. This overlap represents the local deformation of the grains. This approach has been frequently used to model many different processes, such as strain localization and earthquakes [20], fragmentation [21], and damage [22].

The repulsive, elastic normal contact force is proportional to the overlap area a between particles. In Figure 1 the configuration of a contact between two particles is presented, P_1 and P_2 represent the intersection points between the polygons; the segment that connects those points gives the contact line $\mathbf{S} = P_1P_2$. This vector defines a coordinate system $(\hat{n}, \hat{t})$ at the contact, where $\hat{t} = \mathbf{S}/|\mathbf{S}|$ and $\hat{n}$ normal to it give the direction of the normal f_n and tangential f_t components of the contact force. As point of application of the contact forces we choose the center of mass of the overlapping area [23], indicated in the figure with the dot inside the shaded zone.

The elastic force at the contact point is calculated:

$$\mathbf{f}^c = -k_n\delta\hat{n} - k_t\xi\hat{t} \tag{1}$$

where k_n and k_t are the normal and tangential contact stiffnesses, respectively. The deformation length δ is calculated in terms of the overlapping area a and the length of the contact line $|\mathbf{S}|$, $\delta = a/|\mathbf{S}|$. The tangential friction force is introduced by an elastic spring whose length is equal to 0 in the case of new contacts, while for old contacts the tangential spring-length is updated as follows,

$$\xi = \xi' + \mathbf{v}_t^c \Delta t_{MD}, \tag{2}$$

where ξ' is the previous length of the spring, Δt_{MD} is the time step of the molecular dynamic simulation, and $\mathbf{v}_t^c$ the tangential component of the relative velocity $\mathbf{v}^c$ at the contact:

$$\mathbf{v}^c = \mathbf{v}_i - \mathbf{v}_j - \mathbf{w}_i \times \mathbf{l}_i + \mathbf{w}_j \times \mathbf{l}_j. \quad (3)$$

$\mathbf{v}_i$ is here the linear velocity and $\mathbf{w}_i$ the angular velocity of the particles in contact. The tangential elastic displacement ξ at the contact may increase during the time that the condition $|f_t^c| < \mu f_n^c$ is satisfied. The sliding condition is enforced keeping constant the tangential force when the Coulomb limit condition $|f_t^c| = \mu f_n^c$ is reached. At this moment the permanent deformation begins.

We also introduce a viscous force at each contact point, which is necessary to maintain the numerical stability of the method and to take into account dissipation during particle's contact.

$$\mathbf{f}_v^c = -m(\nu_n \cdot \mathbf{v}_n^c \cdot \hat{n}^c - \nu_t \cdot \mathbf{v}_t^c \cdot \hat{t}^c) \quad (4)$$

where $m = (1/m_i + 1/m_j)^{-1}$ is the effective mass (kg) of the two particles in contact, and ν_n and ν_t are damping coefficients. Directly related to the restitution coefficients of the collisions [20]. A background damping force of the form $\mathbf{f}_i^b = -m\nu_b(\mathbf{v}_i + \mathbf{w}_i)$ is also introduced, where ν_b is the background damping coefficient. This background damping force is introduced in order to model the friction between the particles and the bottom (or top) of the shear cell used on the two-dimensional experiments performed by Veje et. al [24], and Howell et al. [25].

2.2 Generation of samples

In order to study the influence of particle shape on the mechanical behavior of granular media, two different types of convex polygons were used to perform the numerical simulations. Figure 2 shows the visual differences between the two types of particles. Polygons depicted in Figure 2(a) with an almost isotropic shape, from now on, will be called 'isotropic' particles, and polygons in 2(b) will be referred as 'elongated' particles. The shape of the particles will be characterized by the aspect ratio λ, which is obtained from the ratio between the length of the longest and shortest axis of the particles.

The random generation of the polygons is accomplished by means of a Voronoi tessellation [26]. A regular square lattice is used to generate the isotropic polygons. This is done by setting a random point in each cell of the lattice. The polygons are constructed by assigning to each point the part of the plane that is nearer to it than to any other point. After generation, particles are moved apart by multiplying their coordinates by a constant in order to obtain a very loose state. Particles are then compressed isotropically by four rigid walls until the desired confining pressure is reached. The elongated particles are generated by stretching or contracting, before the compression, the particles in horizontal or/and vertical direction by a given factor. The average elongation of the grains is given by the ratio between these factors λ (aspect ratio). In our numerical simulations we consider two aspect ratios: $\lambda = 1.0$ for isotropic and $\lambda = 2.3$ for elongated polygons (which are clearly anisotropic). Although aspect ratios larger than 2.3 can be used, we choose this value in order to avoid particles with very sharp angles that could have an unrealistic overlap. Nevertheless, this should be verified by means of a systematic study of different and/or larger aspect ratios of the particles. Finally, by setting the interparticle friction to zero during the compression we obtain the dense samples used in our simulations.

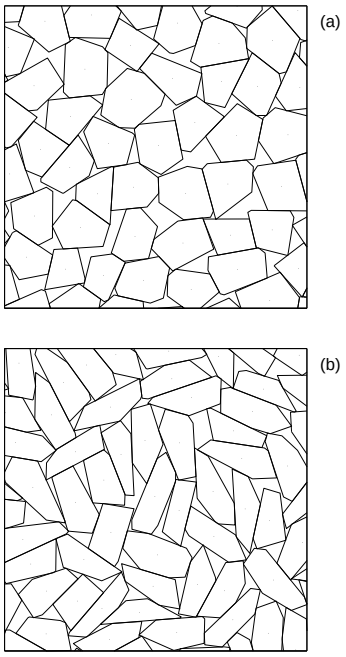

Fig. 2 Two types of particles used in the numerical simulations: (a) isotropic $\lambda = 1.0$ and (b) elongated polygons $\lambda = 2.3$. Points are the center of mass of the polygons.

2.3 Numerical experiment

We want to study the behavior of the granular media in a periodic shear cell. The cell contains 1500 particles, being 50 particle diameters wide and 30 diameters high. Periodic boundary conditions are imposed in horizontal direction. The top and bottom have fixed boundary conditions. A constant confining stress (or normal force) is imposed between the bottom and the top horizontal walls. The top and bottom layers of particles are sheared in opposite direction with a fixed horizontal velocity v_x relative to each other. The particles in one layer are not allowed to rotate or move against each other. The top

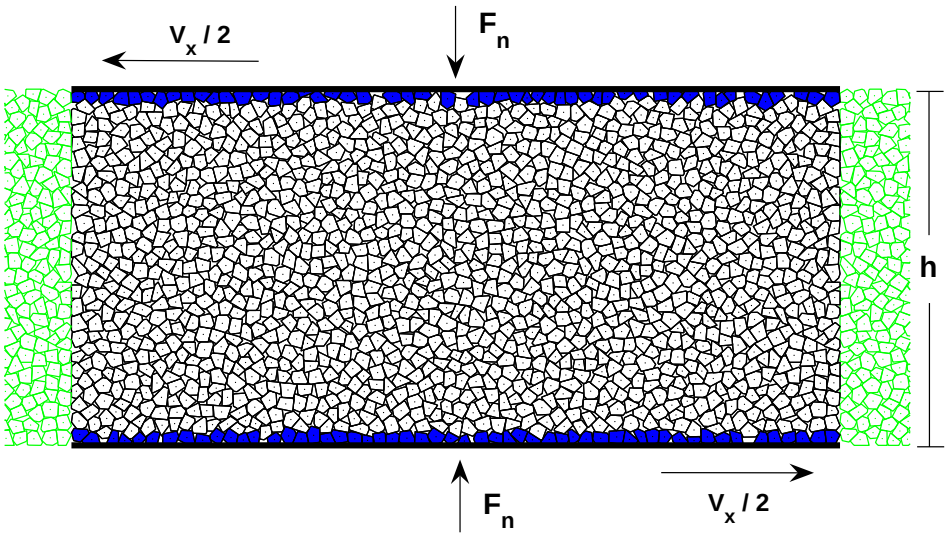

Fig. 3 Sketch of the shear cell. A normal force is applied between top and bottom wall. A horizontal velocity v_x is fixed shearing the sample. Green (grey) particles correspond to the image used to implement the periodic boundary conditions.

boundary is free to move in vertical direction in order to permit a volumetric change of the sample, while the bottom is kept fixed. A configuration of the shear cell used in our simulations is depicted in Figure 3.

In all simulations the mechanical parameters of the particles are: interparticle friction coefficient $\mu = 0.5$, normal stiffness at the contact $k_n = 1.6 \cdot 10^8$ N/m, and normal damping coefficient $\nu_n = 4000$ s^{-1}. The stiffness ratio $\zeta = k_t/k_n$ as well as the viscosity ratio ν_t/ν_n were taken to be 1/3. A background damping coefficient ν_b = 12 s^{-1} was used. Further simulations, results not presented here, with no and different background damping coefficients ν_b in order to evaluate its influence on the mechanical behavior of the medium were performed. We found that the damping ν_b in the range used here has no effect on the evolution of the internal variables of the medium, and additionally that the ν_b value used in this work has no influence on the global mechanical response either.

The horizontal and vertical directions are indicated as x and y, respectively. In order to study the evolution of the packing we use the strain variable γ, which is defined as follows:

$$\gamma = D_x/h_o, \tag{5}$$

where D_x is the horizontal displacement of the boundary particles and h_o is the initial height of the sample. The void ratio e of the sample is related to the volumetric deformation, and is calculated:

$$e = V_T/V_S - 1, \tag{6}$$

where V_T is the total volume of the sample and V_S the volume occupied by all the particles.

3 Shear test simulations

3.1 Global mechanical behavior (effect of initial configuration).

3.1.1 Statistically different samples

Samples corresponding to different seeds for the random number generation of the Voronoi tesellation are used to evaluate the global mechanical response of the granular packing. This is done in order to assess whether different initial configurations of particles reach the same steady state. Our results correspond to a shear velocity of 10 cm/s, and to elongated polygons initially oriented perpendicular to shear direction. In Figure 4 the evolution of the resultant shear force and the void ratio is presented for the different configurations. In Figure 4(a), the shear force F_s is normalized by the normal force F_n applied to the system. Initially, the ratio F_s/F_n has a strong increment related to the breaking of the interlocking of the particles. After this stage, a saturation towards a nearly constant value of the F_s/F_n ratio necessary to shear the granular media is observed, this behavior is identical for all the samples. For small values of strain, the evolution of the void ratio (Figure 4b) also presents a high initial increase saturating later at a constant value. This saturation occurs slower than for F_s/F_n. Samples with elongated particles saturate at a higher value of F_s/F_n and also higher void ratio, as a consequence of the stronger interlocking due to the particle shape. One can therefore conclude that elongated grains are more sensitive to volumetric changes and develop a higher shear strength. This result had been in fact previously observed [11; 12]. We consider this saturation of the F_s/F_n value and void ratio e as the steady state of the sheared material.

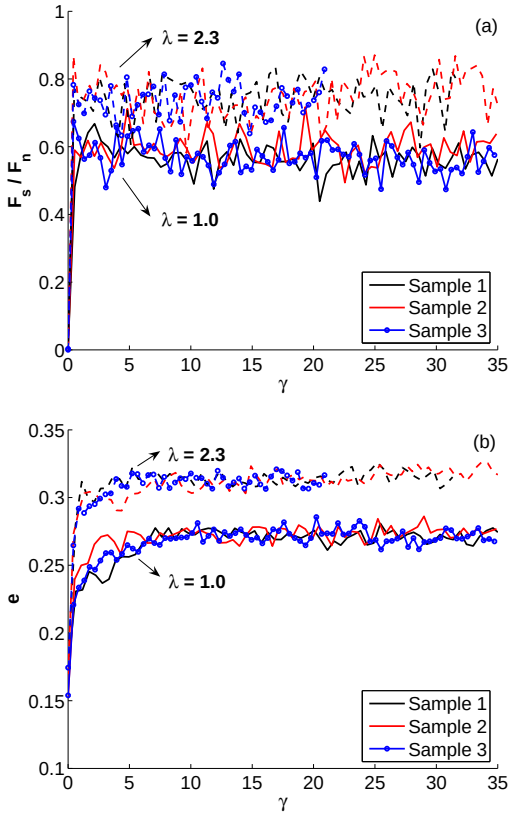

Fig. 4 Evolution of (a) shear force and (b) void ratio for different samples with the same mechanical parameters. Isotropic ($\lambda = 1.0$) and elongated particles ($\lambda = 2.3$) are represented by solid and dashed lines, respectively.

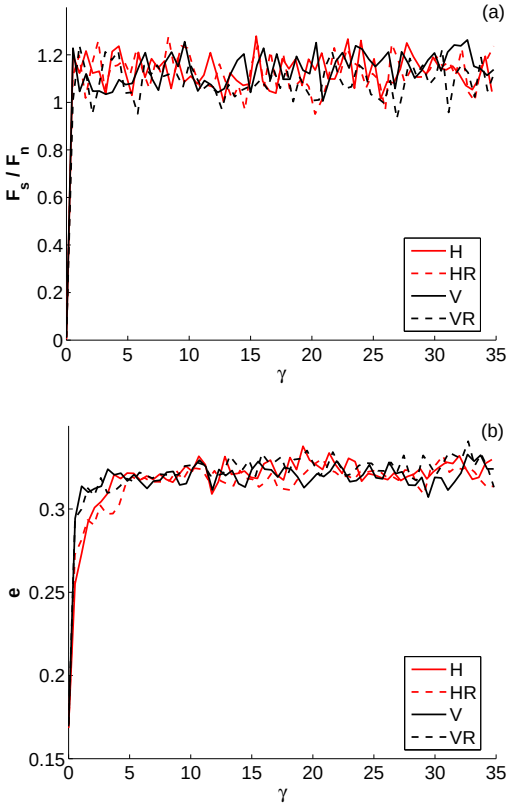

Fig. 6 Evolution of (a) shear force and (b) void ratio for samples with different initial particle orientation, $\lambda = 2.3$. Samples labelled H and V have particles oriented in horizontal and vertical direction, respectively. R corresponds to an initial random rotation of the particles.

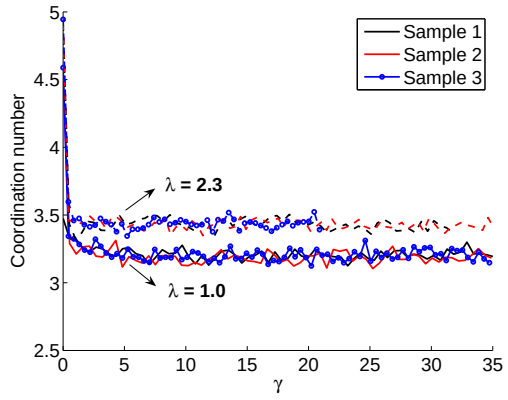

Fig. 5 Evolution of the coordination number for different samples with the same mechanical parameters. Isotropic particles $\lambda = 1.0$ (solid lines) and elongated ones $\lambda = 2.3$ (dashed lines).

The evolution of the coordination number for isotropic and elongated particles is depicted in Figure 5. Note that, despite of reaching a higher void ratio, samples with elongated particles saturate at larger value of coordination number compared to isotropic particles. This can be understood in terms of a geometrical effect, consequence of the flat shape and/or larger relative plane surface in the $\lambda = 2.3$ case, which allows for a higher number of contacts per particle.

3.1.2 Different initial particle orientations

We study in this Section the influence of the anisotropy on the macroscopic behavior of granular media due to the initial orientation of elongated particles. Three different initial configurations are obtained for the samples used in this analysis:

1. On average the grains are oriented parallel to the shear direction (this will be called "horizontal" sample - H).
2. On average the grains are oriented perpendicular to the shear direction (we will call this the "vertical" sample - V).
3. Grains (H or V) are randomly rotated before isotropic compression (which we call the "random" samples - HR or VR).

Configurations number 1 and 2 correspond to samples with different initial orientation of the particles. Config-

uration number 3 is equal to configurations 1 and 2, but with an additional induced random rotation to the particles before the compression (between 0 and 2π *rad*). In all three cases the samples wind up having a slight deviation from the originally induced anisotropy due to particle interactions during the compression.

In Figure 6, the evolution of F_s/F_n and the void ratio e for samples with particles initially oriented in horizontal and vertical direction, and an additional random rotation is presented. Results correspond to a shear velocity of 40 cm/s. We notice that F_s/F_n and the void ratio e evolve toward the same saturation value when they reach the steady state independently of the initial anisotropy due to contact and particle orientations. This independence of the initial anisotropy will be explained by studying the evolution of the internal variables in Section 3.2.

3.2 Evolution of internal variables

In order to get a better understanding of what is occurring at the micro-mechanical level and to find some explanations for the macro-mechanical behavior observed in the previous section, we study the evolution of the local stress, the fabric and the inertia tensors of the samples. Three samples are used: one with isotropic polygons, and two with elongated polygons (corresponding to an initial horizontal and vertical orientation of the particles, as explained in the previous section). Before showing these results, some key concepts that will be required for the description of the media are introduced.

3.2.1 Definitions

The anisotropy of the contact network within the granular sample can be characterized by the fabric tensor of second order $\mathbf{F}$. The fabric tensor takes into account the distribution of the orientations of the contacts between particles, that is to say the geometrical structure of the medium [3]. For a single particle p its components F_{ij} are obtained from

$$F_{ij}^p = \sum_{c=1}^{C^p} l_i^c l_j^c \tag{7}$$

where the dyadic product of the so-called branch vector l^c, connecting the center of mass of the particle to the contact point c, is summed over all the contacts C_p of particle p. Note that, so defined, the trace of the fabric tensor F_{ii}^p is then the number of contacts C_p of the particle p. It is also possible to define a normalized fabric tensor F_{ij}^p/C_p, whose trace is unity. Finally, the mean fabric tensor for an assembly can then be defined as follows:

$$F_{ij} = \frac{1}{N_p} \sum_{p=1}^{N_p} F_{ij}^p \tag{8}$$

where the particle fabric tensor F_{ij}^p is summed over the total number of particles N_p within a representative volume element (RVE). The trace of this tensor is the local mean coordination number C_m, and therefore the normalized mean fabric tensor can also be defined as F_{ij}/C_m.

The inertia tensor can be calculated for each particle as follows:

$$i_{ij}^p = \int \rho(\delta_{ij} \sum_k x_k^2 - x_i x_j) dA \tag{9}$$

where ρ is the density of the particles (kg/m^2), δ_{ij} is the Kronecker delta symbol, k runs in our two-dimensional case from 1 to 2, dA is the differential area element, and x is the shortest distance from the rotation axis to dA.

The mean inertia tensor is calculated in terms of (9):

$$I_{ij} = \frac{1}{N_p} \sum_{p=1}^{N_p} i_{ij}^p \tag{10}$$

where the particle inertia tensor i_{ij}^p is summed over the total number of particles N_p in the RVE.

We also calculate the stress tensor, which is defined in terms of the contact force f_j^c between the grains (acting at the contact point c), and the branch vector l_i^c belonging to the contact point. The stress tensor is defined as follows [27]:

$$\sigma_{ij} = \frac{1}{V} \sum_{c=1}^{N_c} l_i^c f_j^c \tag{11}$$

where V is the volume of the RVE, and the summatory extends over all the contacts N_c in the RVE.

Finally, we will compute the principal directions (major M and minor m) of the mean fabric $\mathbf{F}$, inertia $\mathbf{I}$ and stress σ tensors. These principal directions are measured with the horizontal axis x. We denote θ_F the major principal direction of the fabric tensor, θ_I the major principal direction of the inertia tensor and θ_σ the one of the stress tensor. We are also interested in the individual orientation of non-isotropic particles. We designate θ^p the angle made by the major principal direction of the inertia tensor i_M^p of the particle p with the horizontal axis x. Therefore, θ^p gives the preferred orientation for each particle of the assembly

3.2.2 Evolution of the internal variables

In Figure 7(a-c), we show the orientational distribution of the branch vectors and the principal directions of the mean fabric tensor (F_M and F_m) for the initial configuration of the samples. Observe that, in the case of isotropic polygons (Fig. 7(a)), the distribution presents no preferred direction within the statistical fluctuations. For elongated polygons (Fig. 7(b-c)), however, one can observe that the major principal component of the fabric

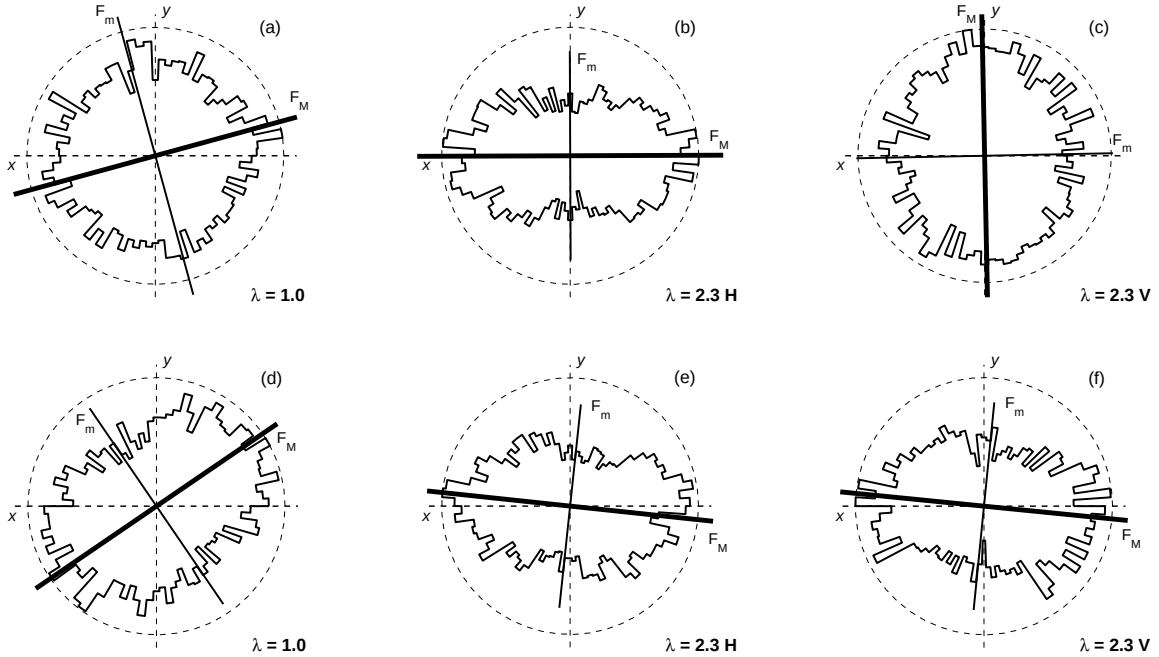

Fig. 7 Polar distribution of branch vectors in the initial configuration (a,b,c) and the steady state (d,e,f), for isotropic particles $\lambda = 1.0$ (a,d), and elongated particles ($\lambda = 2.3$) initially oriented in horizontal direction (b,e) and in vertical direction (c,f). The principal directions of the mean fabric tensor (F_M and F_m), and the reference axes x and y are plotted with solid and dashed lines, respectively. The radius of the dashed circle corresponds to the maximum value of the distribution.

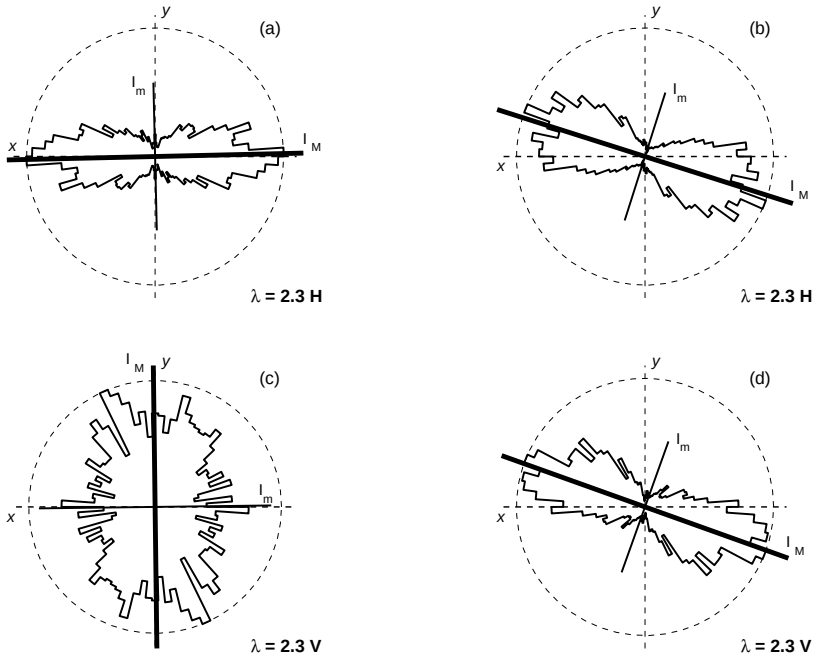

Fig. 8 Polar distribution of particle orientations θ^p, initial configuration (a,c) and in the steady state (b,d) for elongated particles ($\lambda = 2.3$) initially oriented in horizontal direction (a,b) and in vertical direction (c,d). The principal directions of the global inertia tensor (I_M and I_m), and the reference axes x and y are plotted with solid and dashed lines, respectively. The radius of the dashed circle corresponds to the maximum value of the distribution

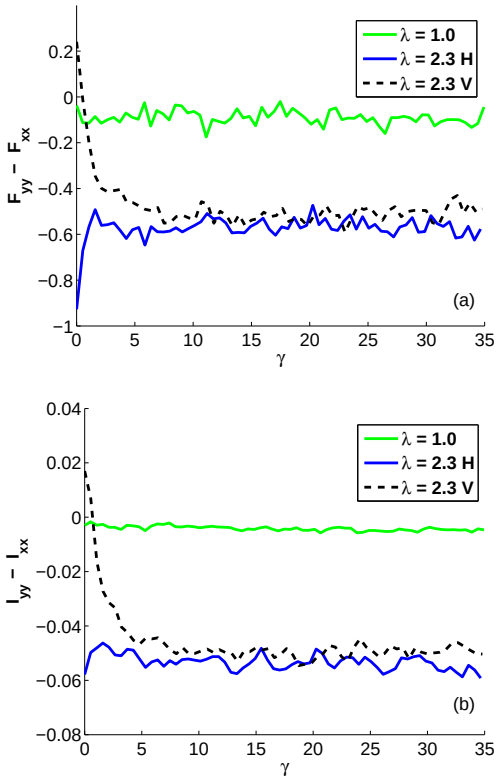

Fig. 9 Evolution of the deviatoric component of the fabric (a) and the inertia tensor (b) for isotropic particles $\lambda = 1.0$, and elongated particles ($\lambda = 2.3$) initially oriented in horizontal direction (H) and in vertical direction (V).

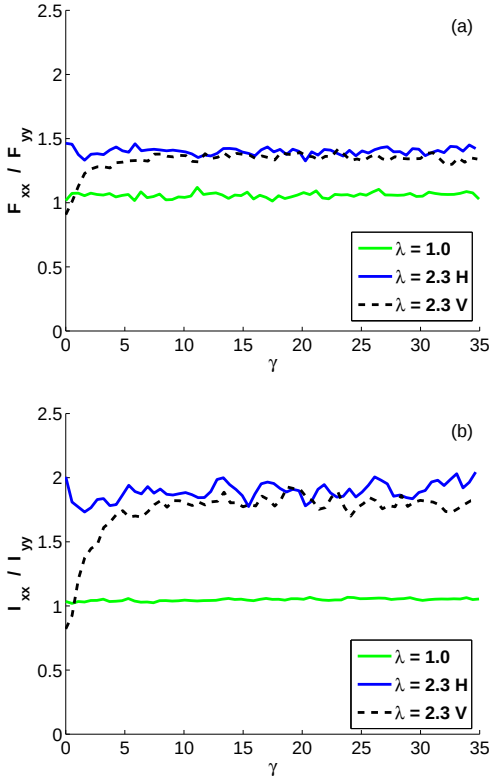

Fig. 10 Evolution of the quotient of the principal components of the fabric (a) and the inertia (b) tensors for isotropic particles $\lambda = 1.0$, and elongated particles ($\lambda = 2.3$) initially oriented in horizontal direction (H) and in vertical direction (V).

tensor **F** is oriented towards the direction in which the polygons were initially stretched.

The anisotropic distribution of the contact orientations is more pronounced in case (b) than in case (c); this is most probably due to the shape of the shear cell (which indeed is wider than higher) and the compression process using rigid walls. The orientational distribution of the contacts in the steady state is depicted in Figure 7(d-f). We notice that the distribution of contact orientations for elongated particles (Fig. 7(e-f)) is very similar independent of their initial orientation, while for isotropic particles (Fig. 7(d)) it is clearly different. The major principal direction of the fabric tensor follows this same trend.

In Figure 8, the polar distribution of θ^p for elongated particles, and the principal directions of the mean inertia tensor (I_M and I_m) in the beginning and in the stationary state are presented. We observe that, similar to the case of contact orientations, they evolve towards the same global orientation independently of the initial particle directions.

In order to study the evolution of the fabric and inertia tensors we monitor their deviatoric component $F_{yy} - F_{xx}$, and the quotient F_{xx} / F_{yy} during the simulation. One can observe in Figure 9, where the evolution of the deviatoric component of F_{ij} and I_{ij} is shown, that the deviatoric reaches a stationary value for both types of particles, and that the induced anisotropy is much higher for elongated particles than for isotropic ones. The same result is observed for the quotient of the principal components of the tensors (Figure 10). This stationary value of the deviatoric component and the quotient is directly related to the steady state at the macro-mechanical level, and seems to be a micro-mechanical requirement for the global steady state. This assumption is supported by simulations of biaxial tests reported by Nouguier-Lehon et al. [11], where samples with elongated particles do not reach neither a stationary value for the components of the fabric and the orientation tensors nor the so-called critical state at the macro-mechanical level, but samples that reach the stationary state for the components of the tensors do so at the global level.

Furthermore, for samples with elongated polygons the deviatoric part of the F_{ij} and I_{ij} tensors, and the ratio of their principal components reach approximately the same stationary value independent of the initial particle orientations. This means that the initial inherent anisotropy (fabric and particle orientation) is completely erased and reoriented in direction of the induced shear

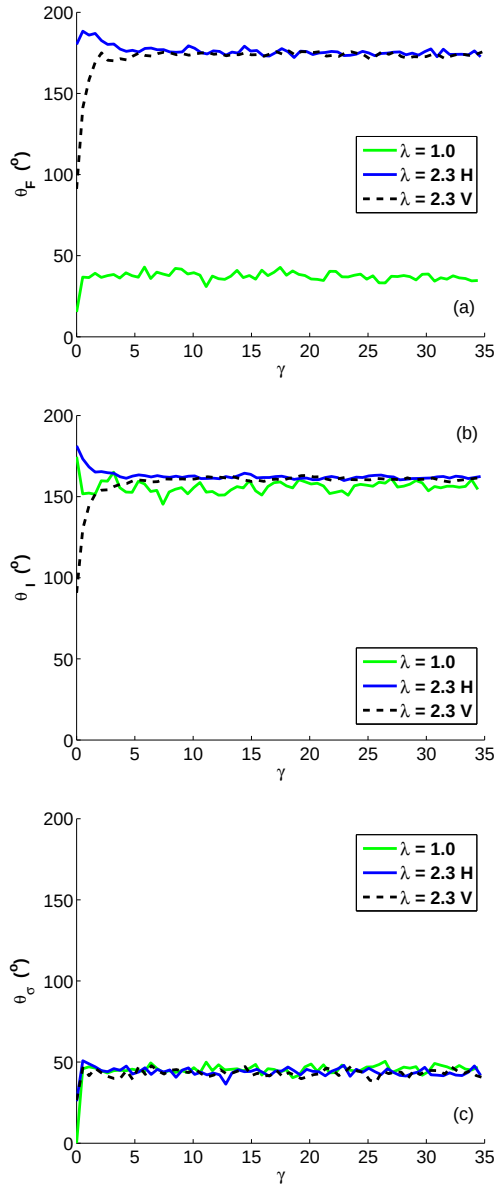

Fig. 11 Evolution of the major principal direction of the fabric (a), the inertia (b), and the stress (c) tensors for isotropic particles $\lambda = 1.0$, and elongated particles ($\lambda = 2.3$) initially oriented in horizontal direction (H) and in vertical direction (V).

during the experiment. The evolution of the major principal direction of the fabric θ_F, the inertia θ_I and the stress tensors θ_σ are shown in Figure 11. In the case of the inertia tensor, the major principal direction θ_I is re-oriented for all samples towards an angle close to 160°. For the stress tensor, θ_σ ($\approx 45°$) is the same for both particles independent of the particle shape. This orientation of the stress comes from the direction of the force chains carrying the largest stresses (Fig. 12(c-d)). On the other hand, the major principal direction of the fabric tensor θ_F is completely different for isotropic and elongated polygons. For isotropic particles it is similar to the major principal direction of stress θ_σ, but for elongated polygons the fabric orientation is close to the one of the inertia tensor.

To clarify this result further, the contact forces larger than the mean value and the principal axes of the fabric tensor of the corresponding particles are plotted in Figure 12. This is done for both types of polygons, and for the initial configuration and a snapshot in the steady state. In Figure 12(a), where the initial configuration of isotropic particles is shown, one can observe that the major principal axis of the fabric tensor of each particle F_M^p is oriented independently of the orientation of the force chains. In the system with elongated particles, however, F_M^p is slightly oriented in the largest dimension of the particles (major principal axis of the tensor of inertia of each particle i_M^p).

In the stationary state, we notice that in the system with isotropic particles F_M^p approximately follows the direction of the force chains that carry the larger forces. In the one with elongated particles, on the contrary, F_M^p is oriented in direction of the largest dimension of the particles i_M^p. The orientation of the elongated particles within the main force chains is associated to the stability of the packing. That is to say; forces are transmitted through contacts closely parallel to the minor principal axis of the inertia tensor of each particle i_m^p, in which flat contact surfaces give a more stable configuration to the system. We conclude then that the orientation of the contacts in the steady state, in the case of non-spherical particles is governed by the particle orientation, and for isotropic particles by the direction of the major principal stress. This is also observed in Figure 11, where in the steady state for isotropic particles θ_F is almost the same as θ_σ, and for elongated particles θ_F is nearly θ_I.

3.3 Shear localization and particle rotation

In order to study strain localization and particle rotation, the shear cell is divided into horizontal layers, i.e parallel to shear direction. For a clearer presentation of the results, we normalize the vertical dimensions with the height of the system h. The origin corresponds to the bottom and 1 to the top of the sample. We use in our analysis the rotation that particles accumulate during every unit increment ($\Delta\gamma_{unit}$) of the strain variable γ in the steady state (in our experiment we take $\gamma_{initial} = 10$ and $\gamma_{final} = 35$, i.e. in total 25 $\Delta\gamma_{unit}$). Then, we average this accumulated particle rotation for each layer of the system, and for all the considered strain increments. In Figure 13, the average accumulated rotation in the steady state for each layer and a shear velocity of 40 cm/s for isotropic and elongated particles initially oriented in vertical direction is shown. We observe a clear localization of rotations, having a peak close to the center and decreasing toward the boundaries. This distribution

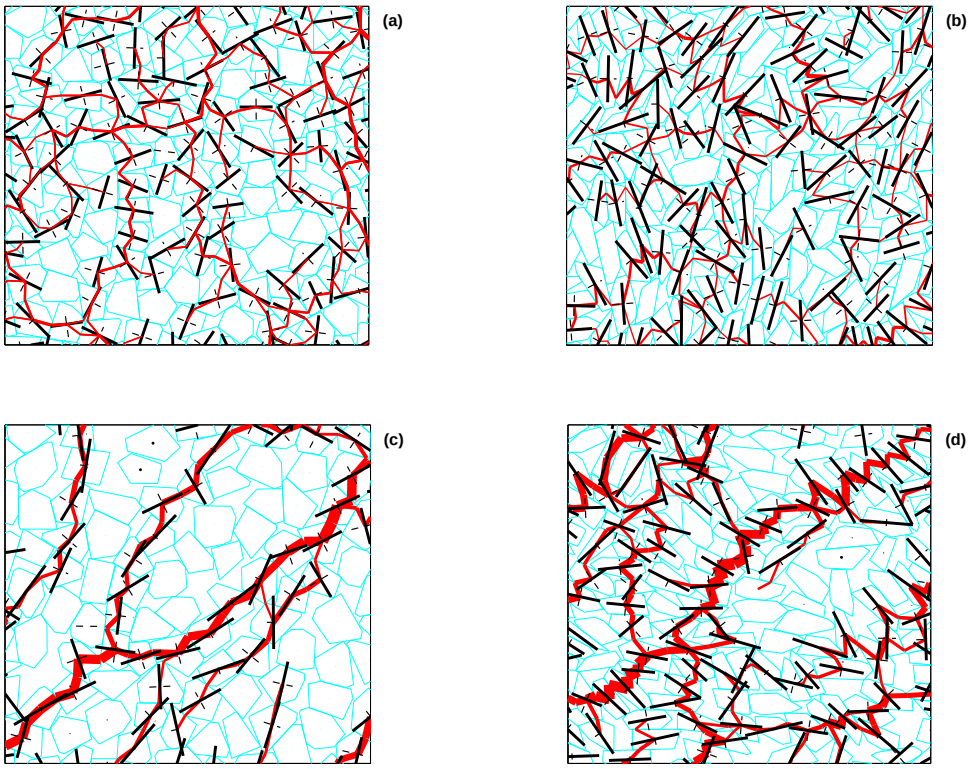

Fig. 12 Force chains (light lines, thickness proportional to magnitude) and principal axes of the fabric tensor (black lines), for initial configuration (a,b) and the steady state (c,d), for isotropic $\lambda = 1.0$ (a,c) and elongated particles $\lambda = 2.3$ (b,d).

resembles the movement of two rigid bodies against each other on a shear band.

We are also interested in the width of the shear zone, which we define here as the width of the zone with particle rotation larger than 80 % of the maximum rotation. One can notice that there are two important differences between the two types of particles considered:

- The average accumulated rotation is lower for elongated particles, in this particular case it is 65 % of the isotropic particles rotation.
- The width of the localization zone is smaller for elongated particles (0.45 times the system height h for elongated and 0.55 times h for isotropic particles).

These differences in accumulated rotation and relative width between isotropic and elongated particles can be explained by the frustration of movement and rotation that elongated particles experience due to the stronger interlocking among them. In this way, the localization zone (rotation zone) for elongated polygons becomes thinner than for isotropic ones. In Figure 14 the mean accumulated rotation since the beginning of the simulation for isotropic and elongated particles is depicted. Notice that the mean rotation is almost twice for isotropic than for elongated particles at the end of the simulation. We also calculate the probability distribution function of particle rotation, which is shown in Figure 15 for both isotropic and elongated particles and $\gamma = 35$. For isotropic particles a more uniform distribution is observed, and the maximum value is close to

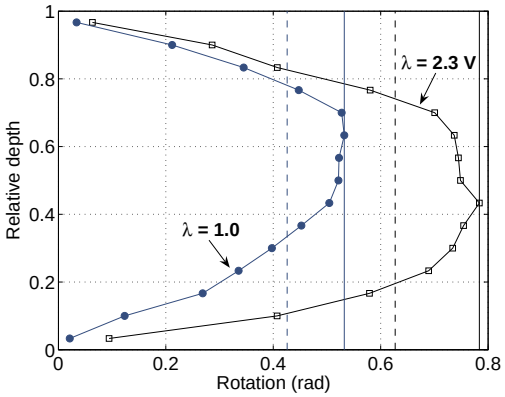

Fig. 13 Average accumulated rotation of the particles during the steady state, isotropic $\lambda = 1.0$ (full dots) and elongated particles $\lambda = 2.3$ V (open squares) within horizontal layers as a function of relative depth. The maximum and 80 % of the maximum value of rotation are plotted as solid and dashed lines, respectively.

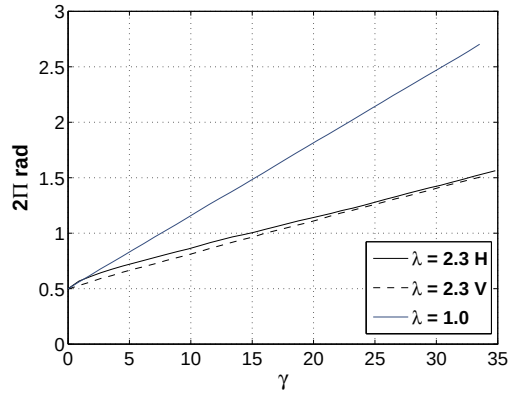

Fig. 14 Mean accumulated rotation since the beginning of the simulation for isotropic particles $\lambda = 1.0$ (light line), and elongated particles ($\lambda = 2.3$) initially oriented in horizontal direction (H, black line), and in vertical direction (V, black-dashed line).

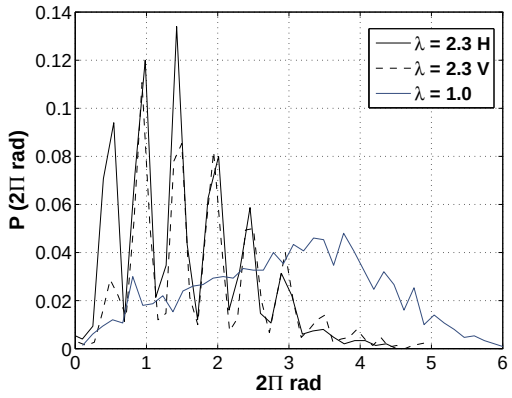

Fig. 15 Probability distribution function of accumulated rotation since the beginning of the simulation until $\gamma = 35$, for isotropic particles ($\lambda = 1.0$, light line), and elongated particles ($\lambda = 2.3$) initially oriented in horizontal direction (black line), and in vertical direction (black-dashed line).

four complete rotations (a complete rotation $2\pi\ rad$). For elongated particles the probability distribution function presents several peaks every half of rotation ($\pi\ rad$). This fact indicates the strong frustration of rotation that such particles undergo during shearing, and that the typical mode of accumulating rotation is then every half complete rotation.

4 Discussion and final remarks

In this paper, the influence of particle shape on the mechanical behavior of sheared dense granular media has been investigated using two-dimensional discrete numerical simulations. Our results show an important influence of particle anisotropy on both the macro and micro-mechanical behavior of the granular media. It is found that for samples with isotropic and elongated particles the shear force and volumetric strain saturate at constant values reaching a steady state. These values in the case of elongated particles are higher than for isotropic particles due to the stronger interlocking between anisotropic particles. This is consequence of the geometrical effect of particle shape. Furthermore, samples with elongated particles reach the same saturation value in the steady state independently of the initial orientation of the particles. This is related to the removal and reorientation of the initial inherent anisotropy (fabric and particle orientations) in direction of the induced shear. This has been confirmed by studying the evolution of the fabric and the inertia tensors.

The deviatoric part and the quotient of the principal components of the fabric $\mathbf{F}$ and inertia $\mathbf{I}$ tensors, for both types of particles, reach a stationary value independent of their initial one. This is directly related to the steady state at the macro-mechanical level. The principal directions of $\mathbf{F}$ and $\mathbf{I}$ present the following behavior: in the initial state of the samples, isotropic polygons present no preferred direction of contacts, however, in the case of elongated polygons the major principal component of $\mathbf{F}$ is oriented along the direction of the major principal component of $\mathbf{I}$. In the steady state, F_M in the case of isotropic particles is reoriented in the direction of the major component of the stress tensor σ, but for elongated particles F_M evolves following the induced orientation that particles undergo during shearing. The direction of the major component of σ is the same for both particle shapes. Independently of the initial orientation, samples with elongated particles reach the same contact θ_F and particle θ_I global orientation in the steady state. One can then conclude that a stationary value of the principal components and principal directions of the fabric and inertia tensors is a micro-mechanical requirement for the existence of the global steady state of the medium. We also conclude that for the sheared dense granular materials here presented, the contact orientation in the global stationary state is governed in the case of isotropic particles by the direction of the major principal component of the stress tensor, and for elongated particles mainly by the major principal component of the inertia tensor (particle orientation).

At the particle level, these results are clearly understood when the inertia and fabric tensor of the particles within the force chains carrying the larger forces are studied. We found that the orientation of elongated particles is associated to the stability of the packing, i.e. forces are transmitted through contacts parallel to the shortest dimension of the particles i_m^p.

Concerning strain localization and particle rotation the following is observed: the width of the shear zone and the accumulated rotation is larger for isotropic particles than for elongated particles. This results is explained by the frustration of rotation that elongated particles experience due to the stronger interlocking among them. This is clearly observed in the probability distribution func-

tion of particle rotation, where the typical mode of accumulating rotation for elongated particles is every π *rad*.

Results presented in this paper lead to a better comprehension of the role of particle shape on the macro and micro-mechanical response of granular materials. It is, however, necessary to say that due to the nature of our two-dimensional analysis, a validation with a three-dimensional model would be very helpful. Further work will focus on a systematic study of the influence of different aspect ratios of the particles, beyond the two limit cases here studied, on the observed phenomena. Additionally, the influence of two types of particles (isotropic and anisotropic) as constituents of the sample on the mechanical behavior of the granular media will be investigated.

Acknowledgements The authors would like to thank F. Alonso-Marroquín for helpful discussions. They also want to acknowledge the support of the *Deutsche Forschungsgemeinschaft* Project HE 2732781 *Micromechanische Untersuchung des granulares Ratchetings* and the EU project Degradation and Instabilities in Geomaterials with Application to Hazard Mitigation (DIGA) in the framework of the Human Potential Program, Research Training Networks (HPRN-CT-2002-00220).

References

1. A. Casagrande and N. Carillo. Shear failure of anisotropic materials. In *Proc. Boston Society of Civil Engrs 31.*, pages 74–78, 1944.
2. M. Oda. Initial fabrics and their relations to mechanical properties of granular materials. *Soils Found.*, 12(1):17–36, 1972.
3. M. Oda, S. Nemat-Nasser, and J. Konishi. Stress-induced anisotropy in granular masses. *Soils Found.*, 25(3):85–97, 1985.
4. M. Oda and H. Nakayama. Introduction of inherent anisotropy of soils in the yield function. In M. Satake and J. T. Jenkins, editors, *Micromechanics of granular materials*, pages 81–90. Elsevier, 1988.
5. X. S. Li and Y. F. Dafalias. Constitutive modeling of inherently anisotropic sand behavior. *J. Geotech. Geoenviron. Engng.*, 128(10):868–880, 2002.
6. E. T. Bowman, K. Soga, and W. Drummond. Particle shape characterization using fourier descriptor analysis. *Géotechnique*, 51(6):545–554, 2001.
7. T. Matsushima and H. Saomoto. Discrete element modeling for irregularly-shaped sand grains. In Mestat, editor, *Proc. NUMGE2002: Numerical Methods in Geotechnical Engineering*, pages 239–246, 2002.
8. E.T Bowman and K. Soga. The influence of particle shape on the stress-strain and creep response of fine silica sand. In R. García-Rojo, H.J. Herrmann, and S. McNamara, editors, *Powders and Grains 2005*, pages 1325–1328. Balkema, 2005.
9. H. M. Shodja and E. G. Nezami. A micromechanical study of rolling and sliding contacts in assemblies of oval granules. *Int. J. Numer. Anal. Meth. Geomech.*, 27:403–424, 2003.
10. C. Nouguier-Lehon and E. Frossard. Influence of particle shape on rotations and rolling movements in granular media. In R. García-Rojo, H.J. Herrmann, and S. McNamara, editors, *Powders and Grains 2005*, pages 1339–1343. Balkema, 2005.
11. C. Nouguier-Lehon, B. Cambou, and E. Vincens. Influence of particle shape and angularity on the behavior of granular materials: a numerical analysis. *Int. J. Numer. Anal. Meth. Geomech.*, 27:1207–1226, 2003.
12. A. A. Peña, A. Lizcano, F. Alonso-Marroquín, and H. J. Herrmann. Investigation of the asymptotic states of granular materials using a discrete model of anisotropic particles. In R. García-Rojo, H.J. Herrmann, and S. McNamara, editors, *Powders and Grains 2005*, pages 697–700. Balkema, 2005.
13. T. T. Ng. Fabric evolution of ellipsoidal arrays with different particle shapes. *ASCE J. Engrg. Mech.*, 127:994–99, 2001.
14. T. T. Ng. Behavior of ellipsoids of two sizes. *J. Geotech. Geoenviron. Engng, ASCE*, 130(10):1077–1083, 2004.
15. Fernando X. Villarruel, Benjamin E. Lauderdale, Daniel M. Mueth, and Heinrich M. Jaeger. Compaction of rods: relaxation and ordering in vibrated, anistopic granular material. *Phys. Rev. E*, 61:6914, 2000.
16. G. Lumay and N. Vandewalle. Compaction of anisotropic granular materials. *Phys. Rev. E*, 70:051314, 2004.
17. P. Ribière, P. Richard, D. Bideau, and R. Delannay. Experimental compaction of anisotropic granular media. *The European Physical Journal E*, 16:415–420, 2005.
18. T. S. Majmudar and R. P. Behringer. Contact force measurements and stress-induced anisotropy in granular materials. *Nature*, 435(23):1079–1082, 2005.
19. M. Lätzel, S. Luding, and H. J. Herrmann. Macroscopic material properties from quasi-static, microscopic simulations of a two-dimensional shear-cell. *Granular Matter*, 2 (3):123–135, 2000.
20. H.-J. Tillemans and H. J. Herrmann. Simulating deformations of granular solids under shear. *Physica A*, 217: 261–288, 1995.
21. F. Kun and H. J. Herrmann. A study of fragmentation processes using a discrete element method. *Comput. Methods Appl. Mech. Eng.*, 138:3–18, 1996.
22. Ferenc Kun and Hans J. Herrmann. Transition from damage to fragmentation in collision of solids. *Phys. Rev. E*, 59(3):2623–2632, 1999.
23. F. Alonso-Marroquin and H.J. Herrmann. Calculation of the incremental stress-strain relation of a polygonal packing. *Phys. Rev. E*, 66:021301, 2002.
24. C. T. Veje, D. W. Howell, and R. P. Behringer. Kinematics of a 2D granular Couette experiment at the transition to shearing. *Phys. Rev. E*, 59:739, 1999.
25. D. Howell, R. P. Behringer, and C. Veje. Stress fluctuations in a 2d granular Couette experiment: A continuous transition. *Phys. Rev. Lett.*, 82:5241, 1999.
26. C. Moukarzel and H. J. Herrmann. A vectorizable random lattice. *Journal of Statistical Physics*, 68:911–923, 1992.
27. L. Rothenburg and A. P. S. Selvadurai. A micromechanical definition of the cauchy stress tensor for particulate media. In A. P. S. Selvadurai, editor, *Mechanics of Structured Media*, pages 469–486. Elsevier, 1981.